



Aaij, R., Adinolfi, M., Bhasin, S., Camargo Magalhaes, P., Chapman, M. G., Kariuki, J. M., Lane, R., Maddrell-Mander, S., Madhan Mohan, L. R., Naik, P., O'Hanlon, D. P., Petridis, K., Pomery, G. J., Velthuis, J. J., Wang, R., Westhenry, B. D. C., Whitehead, M., Zunica, G., al., E., & LHCb Collaboration (2020). Model-independent study of structure in $B^+ \rightarrow D^+ D^- K^+$ decays. *Physical Review Letters*, 125(24), [242001]. <https://doi.org/10.1103/PhysRevLett.125.242001>

Publisher's PDF, also known as Version of record

License (if available):
CC BY

Link to published version (if available):
[10.1103/PhysRevLett.125.242001](https://doi.org/10.1103/PhysRevLett.125.242001)

[Link to publication record in Explore Bristol Research](#)
PDF-document

This is the final published version of the article (version of record). It first appeared online via American Physical Society at <https://journals.aps.org/prl/abstract/10.1103/PhysRevLett.125.242001>. Please refer to any applicable terms of use of the publisher.


University of Bristol - Explore Bristol Research

General rights

This document is made available in accordance with publisher policies. Please cite only the published version using the reference above. Full terms of use are available: <http://www.bristol.ac.uk/red/research-policy/pure/user-guides/ebr-terms/>

Model-Independent Study of Structure in $B^+ \rightarrow D^+ D^- K^+$ Decays

R. Aaij *et al.**
(LHCb Collaboration)

 (Received 2 September 2020; accepted 7 October 2020; published 7 December 2020)

The only anticipated resonant contributions to $B^+ \rightarrow D^+ D^- K^+$ decays are charmonium states in the $D^+ D^-$ channel. A model-independent analysis, using LHCb proton-proton collision data taken at center-of-mass energies of $\sqrt{s} = 7, 8, \text{ and } 13$ TeV, corresponding to a total integrated luminosity of 9 fb^{-1} , is carried out to test this hypothesis. The description of the data assuming that resonances only manifest in decays to the $D^+ D^-$ pair is shown to be incomplete. This constitutes evidence for a new contribution to the decay, potentially one or more new charm-strange resonances in the $D^- K^+$ channel with masses around $2.9 \text{ GeV}/c^2$.

DOI: [10.1103/PhysRevLett.125.242001](https://doi.org/10.1103/PhysRevLett.125.242001)

The $B^+ \rightarrow D^{(*)+} D^{(*)-} K^+$ family of decays offers unique opportunities to study charmonium states. The constrained environment of B -meson decays allows the masses, widths, and quantum numbers of such states to be determined using amplitude analysis techniques, with low backgrounds from other processes. In particular, resonances in the $D^{(*)-} K^+$ or $D^{(*)+} K^+$ channels would be manifestly exotic, having minimal quark content $\bar{c} d u \bar{s}$ or $c \bar{d} u \bar{s}$, respectively. While many exotic hadrons containing $c \bar{c}$ or $b \bar{b}$ quarks have recently been observed [1–3], there is to date no significant evidence of the existence of exotic hadrons with open flavor, i.e., with nonzero strangeness, charm, or beauty quantum numbers. Studies of $B^+ \rightarrow D^{(*)+} D^{(*)-} K^+$ decays are therefore expected to help resolve open questions regarding charmonium spectroscopy [4,5]. In addition, measurements of these processes have been proposed as a method to aid characterization of the $c \bar{c}$ contribution in $B^+ \rightarrow K^+ \mu^+ \mu^-$ decays [6,7].

The branching fractions of $B^+ \rightarrow D^{(*)+} D^{(*)-} K^+$ decays have been measured [8,9], but no prior analyses of their resonant structure exist [10]. Recent studies have shown that extremely pure samples of these decays can be obtained using LHCb data [9] with yields much larger than those available at previous experiments.

A model-dependent study of the resonant structure in $B^+ \rightarrow D^+ D^- K^+$ decays [11], carried out in parallel to this work, has revealed structure in the $D^- K^+$ invariant-mass spectrum that cannot be described by reflections of

charmonium resonances. This highly surprising observation, along with the limited current knowledge of the charmonium spectrum in this mass range, particularly among spin-0 and spin-2 states, motivates the study of this decay using a model-independent approach as presented in this Letter. This method is particularly useful when applied to three-body decays where resonances are only expected to form between one pair of the final-state particles, such that the decay kinematics are described through one mass and one angular variable. Unexpected exotic contributions to the decay process manifest as high-order moments in the distribution of the angular variable, as has been demonstrated by the use of the method to identify exotic resonances contributing to $B^0 \rightarrow \psi(2S) K^+ \pi^-$ [12], $\Lambda_b^0 \rightarrow J/\psi p K^-$ [13], and $B^0 \rightarrow J/\psi K^+ \pi^-$ [14] decays.

The model-independent analysis of the $B^+ \rightarrow D^+ D^- K^+$ decay involves consideration of the distribution of the variable $h(D^+ D^-)$ defined as the cosine of the $D^+ D^-$ helicity angle, i.e., the angle between the momenta of the K^+ and D^- particles in the $D^+ D^-$ rest frame. A description of the $B^+ \rightarrow D^+ D^- K^+$ Dalitz plot is obtained by decomposing the $h(D^+ D^-)$ distribution in terms of Legendre polynomials. The decomposition is done within slices of the $D^+ D^-$ invariant mass, $m(D^+ D^-)$, thereby accounting for the two degrees of freedom in the $B^+ \rightarrow D^+ D^- K^+$ decay kinematics. The description can be projected onto the other invariant-mass distributions in order to identify regions where exotic contributions are needed, and the significance of such deviations can be quantified. If only $D^+ D^-$ resonances contribute, the projections will be well described using only low-order moments up to twice the maximum spin of the charmonium resonances present. If peaking contributions from other channels enter, higher-order moments will be required. The narrower the structure, the higher the order that will be needed. Consequently, a

*Full author list given at the end of the article.

Published by the American Physical Society under the terms of the [Creative Commons Attribution 4.0 International license](https://creativecommons.org/licenses/by/4.0/). Further distribution of this work must maintain attribution to the author(s) and the published article's title, journal citation, and DOI. Funded by SCOAP³.

description employing only low-order moments will be incomplete.

This method is applied to a sample of $B^+ \rightarrow D^+D^-K^+$ candidates selected from LHCb proton-proton (pp) collision datasets, corresponding to integrated luminosities of 3 fb^{-1} recorded during 2011 and 2012 (Run 1) and 6 fb^{-1} from 2015 to 2018 (Run 2). The data sample, selection criteria, background, and efficiency modeling are identical to those in the amplitude analysis of the same process, described in detail in Ref. [11] and briefly summarized here. The LHCb detector [15,16] is a single-arm forward spectrometer covering the pseudorapidity range $2 < \eta < 5$ that is designed for the study of particles containing b or c quarks. Simulation, produced with the software packages described in Refs. [17–20], is used to model the effects of the detector acceptance and the imposed selection requirements. The online event selection is performed by a trigger [21], which consists of a hardware stage, based on information from the calorimeter and muon systems, followed by a software stage, which applies a full event reconstruction and which identifies a two-, three-, or four-track secondary vertex by means of a multivariate algorithm. The charm mesons are reconstructed via the $D^+ \rightarrow K^- \pi^+ \pi^+$ decay. Reconstructed $B^+ \rightarrow D^+D^-K^+$ candidates that pass the trigger criteria are subjected to further selection requirements, including the use of a boosted decision tree (BDT) algorithm [22,23] to reduce the combinatorial background. Variables characterizing the particular topology of the decay (flight distance of the D mesons and displacement of the reconstructed intermediate- and final-state particles from the B production point) and particle identification information are used as inputs to the BDT algorithm. Specific requirements are imposed to suppress contributions from B decays involving one or no D mesons but having the same set of final-state pions and kaons as the signal decays; inspection of the sidebands of the D candidates' invariant-mass distributions confirms that any residual background from this source is at a negligible level.

An extended maximum-likelihood fit is applied to the invariant-mass distribution, $m(D^+D^-K^+)$, of the selected candidates shown in Fig. 1(a). There are 1260 candidates

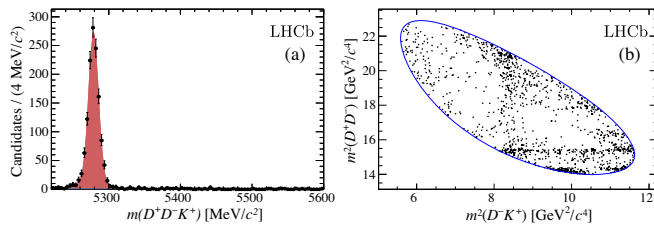


FIG. 1. Invariant-mass distribution for B candidates with the results of the fit superimposed, where the signal component is indicated in red and background (barely visible) in blue (a). Dalitz plot for candidates with $m(D^+D^-K^+)$ values in the signal window (b).

inside the signal window of $m(D^+D^-K^+)$ within $20 \text{ MeV}/c^2$ of the known B^+ mass [24] in which the sample purity is greater than 99.5% and the residual background is combinatorial in nature. The distribution of these candidates, which are retained for further analysis, in the Dalitz plot is shown in Fig. 1(b). The Dalitz-plot coordinates, $m^2(D^-K^+)$ and $m^2(D^+D^-)$, are determined after refitting the candidate decays, imposing the constraints that the reconstructed B^+ and D^\pm masses should match their known values and that the reconstructed B^+ meson should originate at its associated primary pp interaction vertex. Charmonium resonances are clearly visible as horizontal bands in the Dalitz plot, but additional structure also appears to be present. A signal efficiency map is determined as a function of position in the Dalitz plot with simulation, where the particle identification response is calibrated using data control samples [25,26]. The efficiency is found to vary with $m(D^+D^-)$ at the $\pm 10\%$ level and to depend only weakly on $h(D^+D^-)$.

The $m(D^+D^-)$ distribution is divided into slices of width $20 \text{ MeV}/c^2$, which is large compared to the resolution but narrower than any expected structure. Within each slice, the distribution of the cosine of the helicity angle is decomposed according to the basis of Legendre polynomials. Including a factor to ensure normalization over the domain -1 to 1 , these are given by

$$P_n[h(D^+D^-)] = \sqrt{\frac{2n+1}{2}} \times 2^n \sum_{r=0}^n [h(D^+D^-)]^r \binom{n}{r} \left(\frac{n+r-1}{n}\right). \quad (1)$$

In bin j of the $m(D^+D^-)$ distribution, the coefficient of the expansion at order k is referred to as the k th unnormalized moment,

$$\langle Y_k^j \rangle = \sum_{l=1}^{N_j^{\text{Data}}} w_l P_k[h_l(D^+D^-)], \quad (2)$$

where the sum is over the N_j^{Data} candidates in that bin, w_l is a weight assigned to each candidate to achieve a background subtraction and efficiency correction, and $h_l(D^+D^-)$ is the value of $h(D^+D^-)$ for candidate l . To probe whether charmonium resonances with spins up to and including J_{max} account for the structures observed in the Dalitz plot, the expansion can be truncated at a given order, $k_{\text{max}} = 2J_{\text{max}}$.

A simulated sample, generated uniformly in the Dalitz plot and weighted using the truncated expansion, is used in order to visualize the description of the $m(D^-K^+)$ and $m(D^+K^+)$ distributions and to compare them to data. The weights applied to the simulated sample are

$$\eta_i = \frac{2}{N_j^{\text{Sim}}} \times \sum_{k=0}^{k_{\text{max}}} \langle Y_k^j \rangle P_k[h_i(D^+D^-)], \quad (3)$$

where i indexes the generated candidates and N_j^{Sim} is the number of candidates in the simulation in bin j of the $m(D^+D^-)$ spectrum, centered on $m_j(D^+D^-)$.

The significance of any deviation between the truncated Legendre polynomial description and the data can be assessed using pseudoexperiments. They are generated according to a probability density function (PDF) constructed as a function of $m(D^+D^-)$ and $h(D^+D^-)$ given a hypothesis H regarding k_{max} ,

$$\begin{aligned} \mathcal{P}[m_j(D^+D^-), h(D^+D^-)|H] \\ = \mathcal{P}[m_j(D^+D^-)]\mathcal{P}[h(D^+D^-)|H, m_j(D^+D^-)]. \end{aligned} \quad (4)$$

The binned PDF $\mathcal{P}[m_j(D^+D^-)]$ is given by

$$\mathcal{P}[m_j(D^+D^-)] = \mathcal{N} \sum_{l=1}^{N_j^{\text{Data}}} w_l, \quad (5)$$

where \mathcal{N} is a normalization factor. The PDF $\mathcal{P}[h(D^+D^-)|H, m_j(D^+D^-)]$ is a function of the moments and Legendre polynomial functions, reproducing the helicity angle dependence in bin j of $m(D^+D^-)$,

$$\begin{aligned} \mathcal{P}[h(D^+D^-)|H, m_j(D^+D^-)] \\ = 1 + \frac{2}{\sum_{l=1}^{N_j^{\text{Data}}} w_l} \sum_{k=1}^{k_{\text{max}}} \langle Y_k^j \rangle P_k[h(D^+D^-)]. \end{aligned} \quad (6)$$

Since reflections of exotic contributions to the D^-K^+ or D^+K^+ channels would produce complicated structure in the $[m(D^+D^-), h(D^+D^-)]$ plane, the most sensitive model-independent test statistic is based on the PDF for $m(D^-K^+)$ or $m(D^+K^+)$. The PDF $\mathcal{P}[h(D^+D^-)|H, m_j(D^+D^-)]$ is projected onto $m(D^-K^+)$ or $m(D^+K^+)$ by generating candidates uniformly in the $[m(D^+D^-), h(D^+D^-)]$ plane and assigning a weight to each according to Eq. (4). A representation of $\mathcal{P}[m(D^-K^+)|H]$ or $\mathcal{P}[m(D^+K^+)|H]$ is then obtained by filling a histogram of $m(D^-K^+)$ or $m(D^+K^+)$ with these weighted candidates, respectively.

A test statistic is constructed to discriminate between the hypothesis, H_0 , that only D^+D^- resonances contribute up to order k_{max} and the hypothesis that allows for contributions from higher-order moments to describe higher-spin or exotic contributions, H_1 . The test statistic, formulated in terms of determining the significance of deviations in the D^-K^+ channel, has the form [27]

$$t = -2 \sum_{l=1}^{N^{\text{Data}}} s_l \log \left\{ \frac{\mathcal{P}[m_l(D^-K^+)|H_0]/I_{H_0}}{\mathcal{P}[m_l(D^-K^+)|H_1]/I_{H_1}} \right\}, \quad (7)$$

where $\mathcal{P}[m_l(D^-K^+)|H]$ is the value of the PDF in the bin of $m(D^-K^+)$ where candidate l is found, s_l is the signal weight effecting a background subtraction [28], and I_H is a normalization factor computed by Monte Carlo integration,

$$I_H = \sum_{l=1}^{N^{\text{Sim}}} \mathcal{P}[m_l(D^-K^+)|H] \epsilon_l, \quad (8)$$

where ϵ_l is the efficiency appropriate for candidate l .

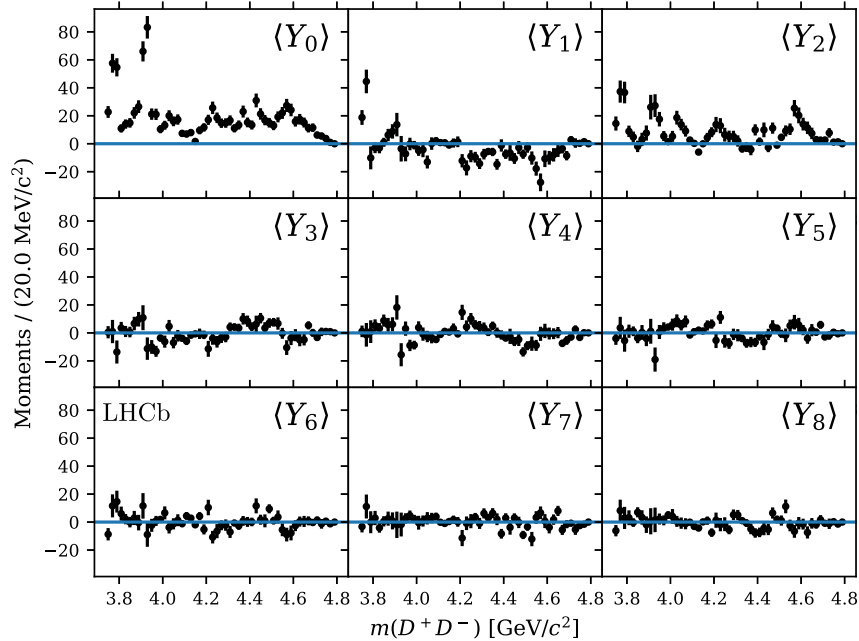


FIG. 2. Distributions of the first nine unnormalized moments, $\langle Y_k^j \rangle$, defined in Eq. (2), as a function of $m(D^+D^-)$ for the selected $B^+ \rightarrow D^+D^-K^+$ candidates after efficiency correction and background subtraction have been applied.

The distributions in the D^+D^- invariant mass $m(D^+D^-)$ of the first nine unnormalized moments defined in Eq. (2) are computed for the selected candidates and are shown in Fig. 2. Significant structure is visible at $m(D^+D^-) \approx 3.8 \text{ GeV}/c^2$ up to and including the second moment, and not at higher orders, as expected for a contribution from the spin-1 resonance $\psi(3770)$. In the vicinity of the $\chi_{c2}(2P)$ resonance near $m(D^+D^-) = 3.9 \text{ GeV}/c^2$, significant structure appears at order 2 and persists, albeit weakly, at order 4. This is found, in the model-dependent analysis [11], to be due to the presence of both spin-0 and spin-2 charmonia in this region. Structure at low $m(D^+D^-)$ in the first moment indicates interference between S and P waves and, similarly, that around $m(D^+D^-) = 3.9 \text{ GeV}/c^2$ in the third moment could indicate interference between P and D waves. Structure apparent at all orders for $m(D^+D^-) > 4.1 \text{ GeV}/c^2$ —though having large uncertainties at orders above 5—could indicate reflection from a structure in another two-body combination.

In order to test how well the $B^+ \rightarrow D^+D^-K^+$ Dalitz plot can be described using a truncated sum over $m(D^+D^-)$ moments, a sample of 10^7 $B^+ \rightarrow D^+D^-K^+$ decays is generated uniformly in the $[m(D^+D^-), h(D^+D^-)]$ plane. Weights are applied according to Eq. (3), and the resulting distribution of the weighted sample is compared to that for the candidates selected from the LHCb data. In the first instance, k_{max} is set to a high value of 29 in the construction of weights to allow all but the smallest of fluctuations in data to be captured. The comparison between the generated decays and the data sample is shown in Fig. 3. The excellent agreement, limited only by statistical fluctuations that can generate structure to arbitrarily high moments, in the $m(D^-K^+)$ and $m(D^+K^+)$ invariant-mass distributions is also to be expected, given the high value of k_{max} .

The effect of truncating the sum over moments at a lower value is explored. A value of $k_{\text{max}} = 4$ is chosen under the assumption that only resonances with spin up to 2 appear in the D^+D^- channel, since production of high-spin resonances in B -meson decays is suppressed and no evidence for a contribution with spin-3 or higher is seen in either Fig. 2 or the model-dependent analysis [11]. Figure 4

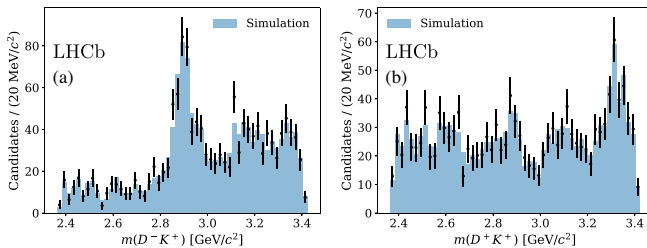


FIG. 3. Comparison between data (points with error bars) and a weighted generated sample (filled histogram) as a function of (a) $m(D^-K^+)$ and (b) $m(D^+K^+)$, where the weights account for the Legendre polynomial moments of orders up to and including 29.

shows the comparison between the weighted generated sample and the data. A prominent discrepancy is apparent around $m(D^-K^+) = 2.9 \text{ GeV}/c^2$. No narrow regions of disagreement are evident in the D^+K^+ spectrum.

The significance of the discrepancy in the $m(D^-K^+)$ distribution between the data and the weighted generated sample in Fig. 4(a) is evaluated using the test statistic defined in Eq. (7). An ensemble of pseudoexperiments, in which each dataset has the same size as the real dataset, is prepared according to the PDF defined in Eq. (6), where k_{max} is taken to be 4. The tiny background contribution is ignored, which introduces negligible uncertainty due to the high purity of the selected $B^+ \rightarrow D^+D^-K^+$ sample. For each pseudoexperiment, a new efficiency map is generated to incorporate the systematic uncertainty arising from the limited size of the simulated sample. This ensemble of nearly 260 000 pseudoexperiments allows determination of the distribution of the test statistic under the hypothesis, H_0 , that only D^+D^- resonances up to spin-2 are present, as shown in Fig. 5. The value of the test statistic obtained from data, t_{Data} , allows the H_0 hypothesis to be rejected at the 99.994% level, corresponding to a significance of 3.9 Gaussian standard deviations (σ). The impact of allowing moments up to order 6 is investigated with a smaller ensemble of nearly 35 000 pseudoexperiments; the significance of the discrepancy remains above 3.7σ .

In summary, a model-independent technique has been employed to confirm whether or not the observed $m(D^-K^+)$ distribution in $B^+ \rightarrow D^+D^-K^+$ decays reconstructed in the LHCb data sample can be explained in terms of reflections from charmonium resonances alone. It is found that the intermediate structure of the decay cannot be described using only D^+D^- resonances of spin up to 2. The significance of the disagreement in the $m(D^-K^+)$ distribution is 3.9σ and is most apparent in the region $m(D^-K^+) = 2.9 \text{ GeV}/c^2$. This discrepancy could be explained by a new, manifestly exotic, charm-strange resonance decaying to the D^-K^+ final state. The outcome of this model-independent study therefore supports the results of the amplitude analysis of the same data [11], where both new spin-0 and spin-1 components are included

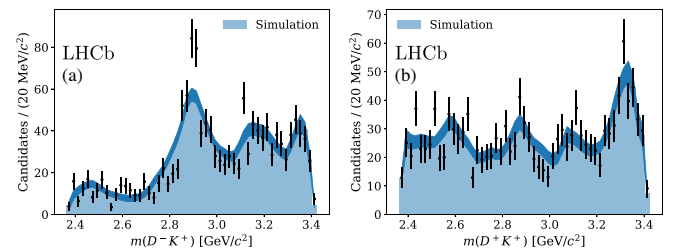


FIG. 4. Comparison between data (points with error bars) and a weighted generated sample (filled histogram) as a function of (a) $m(D^-K^+)$ and (b) $m(D^+K^+)$, where the weights account for the Legendre polynomial moments of orders up to and including 4. The uncertainty on the weighted shape (dark band) is also shown.

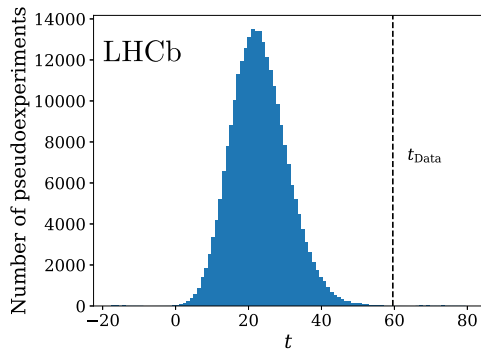


FIG. 5. Comparison of the test statistic evaluated for the data (black dashed line) and for the ensemble of pseudoexperiments (blue histogram) generated according to the PDF constructed using the first four moments of the $h(D^+D^-)$ distribution in data.

in the D^-K^+ channel, as well as $\psi(3770)$, $\chi_{c0}(3930)$, $\chi_{c2}(3930)$, $\psi(4040)$, $\psi(4160)$, and $\psi(4415)$ resonances decaying to D^+D^- , and a nonresonant component.

We express our gratitude to our colleagues in the CERN accelerator departments for the excellent performance of the LHC. We thank the technical and administrative staff at the LHCb institutes. We acknowledge support from CERN and from the national agencies: CAPES, CNPq, FAPERJ, and FINEP (Brazil); MOST and NSFC (China); CNRS/IN2P3 (France); BMBF, DFG, and MPG (Germany); INFN (Italy); NWO (Netherlands); MNiSW and NCN (Poland); MEN/IFA (Romania); MSHE (Russia); MICINN (Spain); SNSF and SER (Switzerland); NASU (Ukraine); STFC (United Kingdom); and DOE NP and NSF (USA). We acknowledge the computing resources that are provided by CERN, IN2P3 (France), KIT, and DESY (Germany), INFN (Italy), SURF (Netherlands), PIC (Spain), GridPP (United Kingdom), RRCKI and Yandex LLC (Russia), CSCS (Switzerland), IFIN-HH (Romania), CBPF (Brazil), PL-GRID (Poland), and OSC (USA). We are indebted to the communities behind the multiple open-source software packages on which we depend. Individual groups or members have received support from AvH Foundation (Germany); EPLANET, Marie Skłodowska-Curie Actions and ERC (European Union); A*MIDEX, ANR, Labex P2IO and OCEVU, and Région Auvergne-Rhône-Alpes (France); Key Research Program of Frontier Sciences of CAS, CAS PIFI, Thousand Talents Program, and Science and Technology Program of Guangzhou (China); RFBR, RSF, and Yandex LLC (Russia); GVA, XuntaGal, and GENCAT (Spain); the Royal Society and the Leverhulme Trust (United Kingdom).

[1] M. Karliner, J. L. Rosner, and T. Skwarnicki, Multiquark states, *Annu. Rev. Nucl. Part. Sci.* **68**, 17 (2018).
 [2] S. L. Olsen, T. Skwarnicki, and D. Zieminska, Nonstandard heavy mesons and baryons: Experimental evidence, *Rev. Mod. Phys.* **90**, 015003 (2018).

[3] A. Ali, J. S. Lange, and S. Stone, Exotics: Heavy pentaquarks and tetraquarks, *Prog. Part. Nucl. Phys.* **97**, 123 (2017).
 [4] S. L. Olsen, Is the $X(3915)$ the $\chi_{c0}(2P)$?, *Phys. Rev. D* **91**, 057501 (2015).
 [5] M.-X. Duan, S.-Q. Luo, X. Liu, and T. Matsuki, Possibility of charmoniumlike state $X(3915)$ as $\chi_{c0}(2P)$ state, *Phys. Rev. D* **101**, 054029 (2020).
 [6] A. Khodjamirian, T. Mannel, A. A. Pivovarov, and Y.-M. Wang, Charm-loop effect in $B \rightarrow K^{(*)}\ell^+\ell^-$ and $B \rightarrow K^*\gamma$, *J. High Energy Phys.* **09** (2010) 089.
 [7] J. Lyon and R. Zwicky, Resonances gone topsy turvy—the charm of QCD or new physics in $b \rightarrow s\ell^+\ell^-$?, [arXiv:1406.0566](https://arxiv.org/abs/1406.0566).
 [8] P. del Amo Sanchez *et al.* (BABAR Collaboration), Measurement of the $B \rightarrow \bar{D}^{(*)}D^{(*)}K$ branching fractions, *Phys. Rev. D* **83**, 032004 (2011).
 [9] R. Aaij *et al.* (LHCb Collaboration), Measurement of the branching fractions for $B^+ \rightarrow D^{*+}D^-K^+$, $B^+ \rightarrow D^{*-}D^+K^+$, and $B^0 \rightarrow D^{*-}D^0K^+$ decays, [arXiv:2005.10264](https://arxiv.org/abs/2005.10264).
 [10] The inclusion of charge-conjugate processes is implied throughout this Letter.
 [11] R. Aaij *et al.* (LHCb Collaboration), companion paper, Amplitude analysis of the $B^+ \rightarrow D^+D^-K^+$ decay, *Phys. Rev. D* **102**, 112003 (2020).
 [12] R. Aaij *et al.* (LHCb Collaboration), Model-independent confirmation of the $Z(4430)^-$ state, *Phys. Rev. D* **92**, 112009 (2015).
 [13] R. Aaij *et al.* (LHCb Collaboration), Model-Independent Evidence for $J/\psi p$ Contributions to $\Lambda_b^0 \rightarrow J/\psi p K^-$ Decays, *Phys. Rev. Lett.* **117**, 082002 (2016).
 [14] R. Aaij *et al.* (LHCb Collaboration), Model-Independent Observation of Exotic Contributions to $B^0 \rightarrow J/\psi K^+\pi^-$ Decays, *Phys. Rev. Lett.* **122**, 152002 (2019).
 [15] A. A. Alves, Jr. *et al.* (LHCb Collaboration), The LHCb detector at the LHC, *J. Instrum.* **3**, S08005 (2008).
 [16] R. Aaij *et al.* (LHCb Collaboration), LHCb detector performance, *Int. J. Mod. Phys. A* **30**, 1530022 (2015).
 [17] T. Sjöstrand, S. Mrenna, and P. Skands, A brief introduction to PYTHIA 8.1, *Comput. Phys. Commun.* **178**, 852 (2008); PYTHIA 6.4 physics and manual, *J. High Energy Phys.* **05** (2006) 026.
 [18] D. J. Lange, The EvtGen particle decay simulation package, *Nucl. Instrum. Methods Phys. Res., Sect. A* **462**, 152 (2001).
 [19] J. Allison *et al.* (Geant4 Collaboration), Geant4 developments and applications, *IEEE Trans. Nucl. Sci.* **53**, 270 (2006); S. Agostinelli *et al.* (Geant4 Collaboration), Geant4: A simulation toolkit, *Nucl. Instrum. Methods Phys. Res., Sect. A* **506**, 250 (2003).
 [20] D. Müller, M. Clemencic, G. Corti, and M. Gersabeck, ReDecay: A novel approach to speed up the simulation at LHCb, *Eur. Phys. J. C* **78**, 1009 (2018).
 [21] R. Aaij *et al.*, The LHCb trigger and its performance in 2011, *J. Instrum.* **8**, P04022 (2013).
 [22] L. Breiman, J. H. Friedman, R. A. Olshen, and C. J. Stone, *Classification and Regression Trees* (Wadsworth International Group, Belmont, CA, 1984).

- [23] J. Stevens and M. Williams, uBoost: A boosting method for producing uniform selection efficiencies from multivariate classifiers, *J. Instrum.* **8**, P12013 (2013).
- [24] M. Tanabashi *et al.* (Particle Data Group), Review of particle physics, *Phys. Rev. D* **98**, 030001 (2018), and 2019 update <https://pdg.lbl.gov/2019/>.
- [25] R. Aaij *et al.*, Selection and processing of calibration samples to measure the particle identification performance of the LHCb experiment in Run 2, *Eur. Phys. J. Tech. Instrum.* **6**, 1 (2018).
- [26] A. Poluektov, Kernel density estimation of a multi-dimensional efficiency profile, *J. Instrum.* **10**, P02011 (2015).
- [27] R. Aaij *et al.* (LHCb Collaboration), Observation of $J/\psi p$ Resonances Consistent with Pentaquark States in $\Lambda_b^0 \rightarrow J/\psi p K^-$ Decays, *Phys. Rev. Lett.* **115**, 072001 (2015).
- [28] M. Pivk and F.R. Le Diberder, sPlot: A statistical tool to unfold data distributions, *Nucl. Instrum. Methods Phys. Res., Sect. A* **555**, 356 (2005).

R. Aaij,³¹ C. Abellán Beteta,⁴⁹ T. Ackernley,⁵⁹ B. Adeva,⁴⁵ M. Adinolfi,⁵³ H. Afsharnia,⁹ C. A. Aidala,⁸⁴ S. Aiola,²⁵ Z. Ajaltouni,⁹ S. Akar,⁶⁴ J. Albrecht,¹⁴ F. Alessio,⁴⁷ M. Alexander,⁵⁸ A. Alfonso Alberio,⁴⁴ Z. Aliouche,⁶¹ G. Alkhazov,³⁷ P. Alvarez Cartelle,⁴⁷ S. Amato,² Y. Amhis,¹¹ L. An,²¹ L. Anderlini,²¹ A. Andreianov,³⁷ M. Andreotti,²⁰ F. Archilli,¹⁶ A. Artamonov,⁴³ M. Artuso,⁶⁷ K. Arzymatov,⁴¹ E. Aslanides,¹⁰ M. Atzeni,⁴⁹ B. Audurier,¹¹ S. Bachmann,¹⁶ M. Bachmayer,⁴⁸ J. J. Back,⁵⁵ S. Baker,⁶⁰ P. Baladron Rodriguez,⁴⁵ V. Balagura,¹¹ W. Baldini,²⁰ J. Baptista Leite,¹ R. J. Barlow,⁶¹ S. Barsuk,¹¹ W. Barter,⁶⁰ M. Bartolini,^{23,a} F. Baryshnikov,⁸⁰ J. M. Basels,¹³ G. Bassi,²⁸ B. Batsukh,⁶⁷ A. Battig,¹⁴ A. Bay,⁴⁸ M. Becker,¹⁴ F. Bedeschi,²⁸ I. Bediaga,¹ A. Beiter,⁶⁷ V. Belavin,⁴¹ S. Belin,²⁶ V. Bellec,⁴⁸ K. Belous,⁴³ I. Belov,³⁹ I. Belyaev,³⁸ G. Bencivenni,²² E. Ben-Haim,¹² A. Berezhnoy,³⁹ R. Bernet,⁴⁹ D. Berninghoff,¹⁶ H. C. Bernstein,⁶⁷ C. Bertella,⁴⁷ E. Bertholet,¹² A. Bertolin,²⁷ C. Betancourt,⁴⁹ F. Betti,^{19,b} M. O. Bettler,⁵⁴ Ia. Bezshyiko,⁴⁹ S. Bhasin,⁵³ J. Bhom,³³ L. Bian,⁷² M. S. Bieker,¹⁴ S. Bifani,⁵² P. Billoir,¹² M. Birch,⁶⁰ F. C. R. Bishop,⁵⁴ A. Bizzeti,^{21,c} M. Björn,⁶² M. P. Blago,⁴⁷ T. Blake,⁵⁵ F. Blanc,⁴⁸ S. Blusk,⁶⁷ D. Bobulska,⁵⁸ J. A. Boelhauve,¹⁴ O. Boente Garcia,⁴⁵ T. Boettcher,⁶³ A. Boldyrev,⁸¹ A. Bondar,^{42,d} N. Bondar,³⁷ S. Borghi,⁶¹ M. Borisyak,⁴¹ M. Borsato,¹⁶ J. T. Borsuk,³³ S. A. Bouchiba,⁴⁸ T. J. V. Bowcock,⁵⁹ A. Boyer,⁴⁷ C. Bozzi,²⁰ M. J. Bradley,⁶⁰ S. Braun,⁶⁵ A. Brea Rodriguez,⁴⁵ M. Brodski,⁴⁷ J. Brodzicka,³³ A. Brossa Gonzalo,⁵⁵ D. Brundu,²⁶ A. Buonaura,⁴⁹ C. Burr,⁴⁷ A. Bursche,²⁶ A. Butkevich,⁴⁰ J. S. Butter,³¹ J. Buytaert,⁴⁷ W. Byczynski,⁴⁷ S. Cadetdu,²⁶ H. Cai,⁷² R. Calabrese,^{20,e} L. Calefice,¹⁴ L. Calero Diaz,²² S. Cali,²² R. Calladine,⁵² M. Calvi,^{24,f} M. Calvo Gomez,⁸³ P. Camargo Magalhaes,⁵³ A. Camboni,⁴⁴ P. Campana,²² D. H. Campora Perez,⁴⁷ A. F. Campoverde Quezada,⁵ S. Capelli,^{24,f} L. Capriotti,^{19,b} A. Carbone,^{19,b} G. Carboni,²⁹ R. Cardinale,^{23,a} A. Cardini,²⁶ I. Carli,⁶ P. Carniti,^{24,f} K. Carvalho Akiba,³¹ A. Casais Vidal,⁴⁵ G. Casse,⁵⁹ M. Cattaneo,⁴⁷ G. Cavallero,⁴⁷ S. Celani,⁴⁸ J. Cerasoli,¹⁰ A. J. Chadwick,⁵⁹ M. G. Chapman,⁵³ M. Charles,¹² Ph. Charpentier,⁴⁷ G. Chatzikonstantinidis,⁵² C. A. Chavez Barajas,⁵⁹ M. Chefdeville,⁸ C. Chen,³ S. Chen,²⁶ A. Chernov,³³ S.-G. Chitic,⁴⁷ V. Chobanova,⁴⁵ S. Cholak,⁴⁸ M. Chrzaszcz,³³ A. Chubykin,³⁷ V. Chulikov,³⁷ P. Ciambone,²² M. F. Cicala,⁵⁵ X. Cid Vidal,⁴⁵ G. Ciezarek,⁴⁷ P. E. L. Clarke,⁵⁷ M. Clemencic,⁴⁷ H. V. Cliff,⁵⁴ J. Closier,⁴⁷ J. L. Cobbedick,⁶¹ V. Coco,⁴⁷ J. A. B. Coelho,¹¹ J. Cogan,¹⁰ E. Cogneras,⁹ L. Cojocariu,³⁶ P. Collins,⁴⁷ T. Colombo,⁴⁷ L. Congedo,¹⁸ A. Contu,²⁶ N. Cooke,⁵² G. Coombs,⁵⁸ G. Corti,⁴⁷ C. M. Costa Sobral,⁵⁵ B. Couturier,⁴⁷ D. C. Craik,⁶³ J. Crkovská,⁶⁶ M. Cruz Torres,¹ R. Currie,⁵⁷ C. L. Da Silva,⁶⁶ E. Dall'Occo,¹⁴ J. Dalseno,⁴⁵ C. D'Ambrosio,⁴⁷ A. Danilina,³⁸ P. d'Argent,⁴⁷ A. Davis,⁶¹ O. De Aguiar Francisco,⁶¹ K. De Bruyn,⁷⁷ S. De Capua,⁶¹ M. De Cian,⁴⁸ J. M. De Miranda,¹ L. De Paula,² M. De Serio,^{18,g} D. De Simone,⁴⁹ P. De Simone,²² J. A. de Vries,⁷⁸ C. T. Dean,⁶⁶ W. Dean,⁸⁴ D. Decamp,⁸ L. Del Buono,¹² B. Delaney,⁵⁴ H.-P. Dembinski,¹⁴ A. Dendek,³⁴ V. Denysenko,⁴⁹ D. Derkach,⁸¹ O. Deschamps,⁹ F. Desse,¹¹ F. Dettori,^{26,h} B. Dey,⁷² P. Di Nezza,²² S. Didenko,⁸⁰ L. Dieste Maronas,⁴⁵ H. Dijkstra,⁴⁷ V. Dobishuk,⁵¹ A. M. Donohoe,¹⁷ F. Dordei,²⁶ A. C. dos Reis,¹ L. Douglas,⁵⁸ A. Dovbnya,⁵⁰ A. G. Downes,⁸ K. Dreimanis,⁵⁹ M. W. Dudek,³³ L. Dufour,⁴⁷ V. Duk,⁷⁶ P. Durante,⁴⁷ J. M. Durham,⁶⁶ D. Dutta,⁶¹ M. Dziewiecki,¹⁶ A. Dziurda,³³ A. Dzyuba,³⁷ S. Easo,⁵⁶ U. Egede,⁶⁸ V. Egorychev,³⁸ S. Eidelman,^{42,d} S. Eisenhardt,⁵⁷ S. Ek-In,⁴⁸ L. Eklund,⁵⁸ S. Ely,⁶⁷ A. Ene,³⁶ E. Eppe,⁶⁶ S. Escher,¹³ J. Eschle,⁴⁹ S. Esen,¹¹ T. Evans,⁴⁷ A. Falabella,¹⁹ J. Fan,³ Y. Fan,⁵ B. Fang,⁷² N. Farley,⁵² S. Farry,⁵⁹ D. Fazzini,^{24,f} P. Fedin,³⁸ M. Féo,⁴⁷ P. Fernandez Declara,⁴⁷ A. Fernandez Prieto,⁴⁵ J. M. Fernandez-tenllado Arribas,⁴⁴ F. Ferrari,^{19,b} L. Ferreira Lopes,⁴⁸ F. Ferreira Rodrigues,² S. Ferreres Sole,³¹ M. Ferrillo,⁴⁹ M. Ferro-Luzzi,⁴⁷ S. Filippov,⁴⁰ R. A. Fini,¹⁸ M. Fiorini,^{20,e} M. Firlej,³⁴ K. M. Fischer,⁶² C. Fitzpatrick,⁶¹ T. Fiutowski,³⁴ F. Fleuret,^{11,i} M. Fontana,⁴⁷ F. Fontanelli,^{23,a} R. Forty,⁴⁷ V. Franco Lima,⁵⁹ M. Franco Sevilla,⁶⁵ M. Frank,⁴⁷ E. Franzoso,²⁰ G. Frau,¹⁶ C. Frei,⁴⁷ D. A. Friday,⁵⁸ J. Fu,²⁵

Q. Fuehring,¹⁴ W. Funk,⁴⁷ E. Gabriel,³¹ T. Gaintseva,⁴¹ A. Gallas Torreira,⁴⁵ D. Galli,^{19,b} S. Gambetta,⁵⁷ Y. Gan,³
 M. Gandelman,² P. Gandini,²⁵ Y. Gao,⁴ M. Garau,²⁶ L. M. Garcia Martin,⁵⁵ P. Garcia Moreno,⁴⁴ J. García Pardiñas,⁴⁹
 B. Garcia Plana,⁴⁵ F. A. Garcia Rosales,¹¹ L. Garrido,⁴⁴ D. Gascon,⁴⁴ C. Gaspar,⁴⁷ R. E. Geertsema,³¹ D. Gerick,¹⁶
 L. L. Gerken,¹⁴ E. Gersabeck,⁶¹ M. Gersabeck,⁶¹ T. Gershon,⁵⁵ D. Gerstel,¹⁰ Ph. Ghez,⁸ V. Gibson,⁵⁴ M. Giovannetti,^{22,j}
 A. Gioventù,⁴⁵ P. Gironella Gironell,⁴⁴ L. Giubega,³⁶ C. Giugliano,^{20,e} K. Gizdov,⁵⁷ E. L. Gkougkousis,⁴⁷ V. V. Gligorov,¹²
 C. Göbel,⁶⁹ E. Golobardes,⁸³ D. Golubkov,³⁸ A. Golutvin,^{60,80} A. Gomes,^{1,k} S. Gomez Fernandez,⁴⁴
 F. Goncalves Abrantes,⁶⁹ M. Goncerz,³³ G. Gong,³ P. Gorbounov,³⁸ I. V. Gorelov,³⁹ C. Gotti,^{24,f} E. Govorkova,³¹
 J. P. Grabowski,¹⁶ R. Graciani Diaz,⁴⁴ T. Grammatico,¹² L. A. Granado Cardoso,⁴⁷ E. Graugés,⁴⁴ E. Graverini,⁴⁸
 G. Graziani,²¹ A. Grecu,³⁶ L. M. Greeven,³¹ P. Griffith,²⁰ L. Grillo,⁶¹ S. Gromov,⁸⁰ L. Gruber,⁴⁷ B. R. Gruber Cazon,⁶²
 C. Gu,³ M. Guarise,²⁰ P. A. Günther,¹⁶ E. Gushchin,⁴⁰ A. Guth,¹³ Y. Guz,^{43,47} T. Gys,⁴⁷ T. Hadavizadeh,⁶⁸ G. Haefeli,⁴⁸
 C. Haen,⁴⁷ J. Haimberger,⁴⁷ S. C. Haines,⁵⁴ T. Halewood-leagas,⁵⁹ P. M. Hamilton,⁶⁵ Q. Han,⁷ X. Han,¹⁶ T. H. Hancock,⁶²
 S. Hansmann-Menzemer,¹⁶ N. Harnew,⁶² T. Harrison,⁵⁹ C. Hasse,⁴⁷ M. Hatch,⁴⁷ J. He,⁵ M. Hecker,⁶⁰ K. Heijhoff,³¹
 K. Heinicke,¹⁴ A. M. Hennequin,⁴⁷ K. Hennessy,⁵⁹ L. Henry,^{25,46} J. Heuel,¹³ A. Hicheur,² D. Hill,⁶² M. Hilton,⁶¹
 S. E. Hollitt,¹⁴ P. H. Hopchev,⁴⁸ J. Hu,¹⁶ J. Hu,⁷¹ W. Hu,⁷ W. Huang,⁵ X. Huang,⁷² W. Hulsbergen,³¹ R. J. Hunter,⁵⁵
 M. Hushchyn,⁸¹ D. Hutchcroft,⁵⁹ D. Hynds,³¹ P. Ibis,¹⁴ M. Idzik,³⁴ D. Ilin,³⁷ P. Ilten,⁵² A. Inglessi,³⁷ A. Ishteev,⁸⁰
 K. Ivshin,³⁷ R. Jacobsson,⁴⁷ S. Jakobsen,⁴⁷ E. Jans,³¹ B. K. Jashal,⁴⁶ A. Jawahery,⁶⁵ V. Jevtic,¹⁴ M. Jezabek,³³ F. Jiang,³
 M. John,⁶² D. Johnson,^{47,†} C. R. Jones,⁵⁴ T. P. Jones,⁵⁵ B. Jost,⁴⁷ N. Jurik,⁴⁷ S. Kandybei,⁵⁰ Y. Kang,³ M. Karacson,⁴⁷
 J. M. Kariuki,⁵³ N. Kazeev,⁸¹ M. Kecke,¹⁶ F. Keizer,^{54,47} M. Kenzie,⁵⁵ T. Ketel,³ B. Khanji,⁴⁷ A. Kharisova,⁸²
 S. Kholodenko,⁴³ K. E. Kim,⁶⁷ T. Kim,¹³ V. S. Kirsebom,⁴⁸ O. Kitouni,⁶³ S. Klaver,³¹ K. Klimaszewski,³⁵ S. Koliiev,⁵¹
 A. Kondybayeva,⁸⁰ A. Konoplyannikov,³⁸ P. Kopciwicz,³⁴ R. Kopečna,¹⁶ P. Koppenburg,³¹ M. Korolev,³⁹ I. Kostiuk,^{31,51}
 O. Kot,⁵¹ S. Kotriakhova,^{37,30} P. Kravchenko,³⁷ L. Kravchuk,⁴⁰ R. D. Krawczyk,⁴⁷ M. Kreps,⁵⁵ F. Kress,⁶⁰ S. Kretschmar,¹³
 P. Krokovny,^{42,d} W. Krupa,³⁴ W. Krzemien,³⁵ W. Kucewicz,^{33,l} M. Kucharczyk,³³ V. Kudryavtsev,^{42,d} H. S. Kuindersma,³¹
 G. J. Kunde,⁶⁶ T. Kvaratskheliya,³⁸ D. Lacarrere,⁴⁷ G. Lafferty,⁶¹ A. Lai,²⁶ A. Lampis,²⁶ D. Lancierini,⁴⁹ J. J. Lane,⁶¹
 R. Lane,⁵³ G. Lanfranchi,²² C. Langenbruch,¹³ J. Langer,¹⁴ O. Lantwin,^{49,80} T. Latham,⁵⁵ F. Lazzari,^{28,m} R. Le Gac,¹⁰
 S. H. Lee,⁸⁴ R. Lefèvre,⁹ A. Leflat,³⁹ S. Legotin,⁸⁰ O. Leroy,¹⁰ T. Lesiak,³³ B. Leverington,¹⁶ H. Li,⁷¹ L. Li,⁶² P. Li,¹⁶ X. Li,⁶⁶
 Y. Li,⁶ Y. Li,⁶ Z. Li,⁶⁷ X. Liang,⁶⁷ T. Lin,⁶⁰ R. Lindner,⁴⁷ V. Lisovskyi,¹⁴ R. Litvinov,²⁶ G. Liu,⁷¹ H. Liu,⁵ S. Liu,⁶ X. Liu,³
 A. Loi,²⁶ J. Lomba Castro,⁴⁵ I. Longstaff,⁵⁸ J. H. Lopes,² G. Loustau,⁴⁹ G. H. Lovell,⁵⁴ Y. Lu,⁶ D. Lucchesi,^{27,n} S. Luchuk,⁴⁰
 M. Lucio Martinez,³¹ V. Lukashenko,³¹ Y. Luo,³ A. Lupato,⁶¹ E. Luppi,^{20,e} O. Lupton,⁵⁵ A. Lusiani,^{28,o} X. Lyu,⁵ L. Ma,⁶
 S. Maccolini,^{19,b} F. Macheferf,¹¹ F. Maciuc,³⁶ V. Macko,⁴⁸ P. Mackowiak,¹⁴ S. Maddrell-Mander,⁵³ O. Madejczyk,³⁴
 L. R. Madhan Mohan,⁵³ O. Maev,³⁷ A. Maevskiy,⁸¹ D. Maisuzenko,³⁷ M. W. Majewski,³⁴ S. Malde,⁶² B. Malecki,⁴⁷
 A. Malinin,⁷⁹ T. Maltsev,^{42,d} H. Malygina,¹⁶ G. Manca,^{26,h} G. Mancinelli,¹⁰ R. Manera Escalero,⁴⁴ D. Manuzzi,^{19,b}
 D. Marangotto,^{25,p} J. Maratas,^{9,q} J. F. Marchand,⁸ U. Marconi,¹⁹ S. Mariani,^{21,47,r} C. Marin Benito,¹¹ M. Marinangeli,⁴⁸
 P. Marino,⁴⁸ J. Marks,¹⁶ P. J. Marshall,⁵⁹ G. Martellotti,³⁰ L. Martinazzoli,⁴⁷ M. Martinelli,^{24,f} D. Martinez Santos,⁴⁵
 F. Martinez Vidal,⁴⁶ A. Massafferri,¹ M. Materok,¹³ R. Matev,⁴⁷ A. Mathad,⁴⁹ Z. Mathe,⁴⁷ V. Matiunin,³⁸ C. Matteuzzi,²⁴
 K. R. Mattioli,⁸⁴ A. Mauri,³¹ E. Maurice,^{11,i} J. Mauricio,⁴⁴ M. Mazurek,³⁵ M. McCann,⁶⁰ L. McConnell,¹⁷ T. H. Mcgrath,⁶¹
 A. McNab,⁶¹ R. McNulty,¹⁷ J. V. Mead,⁵⁹ B. Meadows,⁶⁴ C. Meaux,¹⁰ G. Meier,¹⁴ N. Meinert,⁷⁵ D. Melnychuk,³⁵
 S. Meloni,^{24,f} M. Merk,^{31,78} A. Merli,²⁵ L. Meyer Garcia,² M. Mikhasenko,⁴⁷ D. A. Milanes,⁷³ E. Millard,⁵⁵
 M. Milovanovic,⁴⁷ M.-N. Minard,⁸ L. Minzoni,^{20,e} S. E. Mitchell,⁵⁷ B. Mitreska,⁶¹ D. S. Mitzel,⁴⁷ A. Mödden,¹⁴
 R. A. Mohammed,⁶² R. D. Moise,⁶⁰ T. Mombächer,¹⁴ I. A. Monroy,⁷³ S. Monteil,⁹ M. Morandin,²⁷ G. Morello,²²
 M. J. Morello,^{28,o} J. Moron,³⁴ A. B. Morris,⁷⁴ A. G. Morris,⁵⁵ R. Mountain,⁶⁷ H. Mu,³ F. Muheim,⁵⁷ M. Mukherjee,⁷
 M. Mulder,⁴⁷ D. Müller,⁴⁷ K. Müller,⁴⁹ C. H. Murphy,⁶² D. Murray,⁶¹ P. Muzzetto,²⁶ P. Naik,⁵³ T. Nakada,⁴⁸
 R. Nandakumar,⁵⁶ T. Nanut,⁴⁸ I. Nasteva,² M. Needham,⁵⁷ I. Neri,^{20,e} N. Neri,^{25,p} S. Neubert,⁷⁴ N. Neufeld,⁴⁷
 R. Newcombe,⁶⁰ T. D. Nguyen,⁴⁸ C. Nguyen-Mau,⁴⁸ E. M. Niel,¹¹ S. Nieswand,¹³ N. Nikitin,³⁹ N. S. Nolte,⁴⁷ C. Nunez,⁸⁴
 A. Oblakowska-Mucha,³⁴ V. Obraztsov,⁴³ D. P. O'Hanlon,⁵³ R. Oldeman,^{26,h} C. J. G. Onderwater,⁷⁷ A. Ossowska,³³
 J. M. Otalora Goicochea,² T. Ovsiannikova,³⁸ P. Owen,⁴⁹ A. Oyanguren,⁴⁶ B. Pagare,⁵⁵ P. R. Pais,⁴⁷ T. Pajero,^{28,47,o}
 A. Palano,¹⁸ M. Palutan,²² Y. Pan,⁶¹ G. Panshin,⁸² A. Papanestis,⁵⁶ M. Pappagallo,^{18,g} L. L. Pappalardo,^{20,e}
 C. Pappenheimer,⁶⁴ W. Parker,⁶⁵ C. Parkes,⁶¹ C. J. Parkinson,⁴⁵ B. Passalacqua,²⁰ G. Passaleva,²¹ A. Pastore,¹⁸ M. Patel,⁶⁰
 C. Patrignani,^{19,b} C. J. Pawley,⁷⁸ A. Pearce,⁴⁷ A. Pellegrino,³¹ M. Pepe Altarelli,⁴⁷ S. Perazzini,¹⁹ D. Pereima,³⁸ P. Perret,⁹
 K. Petridis,⁵³ A. Petrolini,^{23,a} A. Petrov,⁷⁹ S. Petrucci,⁵⁷ M. Petruzzo,²⁵ A. Philippov,⁴¹ L. Pica,²⁸ M. Piccini,⁷⁶ B. Pietrzyk,⁸

G. Pietrzyk,⁴⁸ M. Pili,⁶² D. Pinci,³⁰ J. Pinzino,⁴⁷ F. Pisani,⁴⁷ A. Piucci,¹⁶ Resmi P. K.,¹⁰ V. Placinta,³⁶ S. Playfer,⁵⁷ J. Plews,⁵² M. Plo Casasus,⁴⁵ F. Polci,¹² M. Poli Lener,²² M. Poliakov,⁶⁷ A. Poluektov,¹⁰ N. Polukhina,^{80,s} I. Polyakov,⁶⁷ E. Polycarpo,² G. J. Pomery,⁵³ S. Ponce,⁴⁷ A. Popov,⁴³ D. Popov,^{5,47} S. Popov,⁴¹ S. Poslavskii,⁴³ K. Prasanth,³³ L. Promberger,⁴⁷ C. Prouve,⁴⁵ V. Pugatch,⁵¹ A. Puig Navarro,⁴⁹ H. Pullen,⁶² G. Punzi,^{28,t} W. Qian,⁵ J. Qin,⁵ R. Quagliani,¹² B. Quintana,⁸ N. V. Raab,¹⁷ R. I. Rabadan Trejo,¹⁰ B. Rachwal,³⁴ J. H. Rademacker,⁵³ M. Rama,²⁸ M. Ramos Pernas,⁵⁵ M. S. Rangel,² F. Ratnikov,^{41,81} G. Raven,³² M. Reboud,⁸ F. Redi,⁴⁸ F. Reiss,¹² C. Remon Alepuz,⁴⁶ Z. Ren,³ V. Renaudin,⁶² R. Ribatti,²⁸ S. Ricciardi,⁵⁶ D. S. Richards,⁵⁶ K. Rinnert,⁵⁹ P. Robbe,¹¹ A. Robert,¹² G. Robertson,⁵⁷ A. B. Rodrigues,⁴⁸ E. Rodrigues,⁵⁹ J. A. Rodriguez Lopez,⁷³ A. Rollings,⁶² P. Roloff,⁴⁷ V. Romanovskiy,⁴³ M. Romero Lamas,⁴⁵ A. Romero Vidal,⁴⁵ J. D. Roth,⁸⁴ M. Rotondo,²² M. S. Rudolph,⁶⁷ T. Ruf,⁴⁷ J. Ruiz Vidal,⁴⁶ A. Ryzhikov,⁸¹ J. Ryzka,³⁴ J. J. Saborido Silva,⁴⁵ N. Sagidova,³⁷ N. Sahoo,⁵⁵ B. Saitta,^{26,h} D. Sanchez Gonzalo,⁴⁴ C. Sanchez Gras,³¹ C. Sanchez Mayordomo,⁴⁶ R. Santacesaria,³⁰ C. Santamarina Rios,⁴⁵ M. Santimaria,²² E. Santovetti,^{29,j} D. Saranin,⁸⁰ G. Sarpis,⁶¹ M. Sarpis,⁷⁴ A. Sarti,³⁰ C. Satriano,^{30,u} A. Satta,²⁹ M. Saur,⁵ D. Savrina,^{38,39} H. Sazak,⁹ L. G. Scantlebury Smead,⁶² S. Schael,¹³ M. Schellenberg,¹⁴ M. Schiller,⁵⁸ H. Schindler,⁴⁷ M. Schmelling,¹⁵ T. Schmelzer,¹⁴ B. Schmidt,⁴⁷ O. Schneider,⁴⁸ A. Schopper,⁴⁷ M. Schubiger,³¹ S. Schulte,⁴⁸ M. H. Schune,¹¹ R. Schwemmer,⁴⁷ B. Sciascia,²² A. Sciubba,³⁰ S. Sellam,⁴⁵ A. Semennikov,³⁸ M. Senghi Soares,³² A. Sergi,^{52,47} N. Serra,⁴⁹ J. Serrano,¹⁰ L. Sestini,²⁷ A. Seuthe,¹⁴ P. Seyfert,⁴⁷ D. M. Shangase,⁸⁴ M. Shapkin,⁴³ I. Shchemerov,⁸⁰ L. Shchutska,⁴⁸ T. Shears,⁵⁹ L. Shekhtman,^{42,d} Z. Shen,⁴ V. Shevchenko,⁷⁹ E. B. Shields,^{24,f} E. Shmanin,⁸⁰ J. D. Shupperd,⁶⁷ B. G. Siddi,²⁰ R. Silva Coutinho,⁴⁹ G. Simi,²⁷ S. Simone,^{18,g} I. Skiba,^{20,e} N. Skidmore,⁷⁴ T. Skwarnicki,⁶⁷ M. W. Slater,⁵² J. C. Smallwood,⁶² J. G. Smeaton,⁵⁴ A. Smetkina,³⁸ E. Smith,¹³ M. Smith,⁶⁰ A. Snoch,³¹ M. Soares,¹⁹ L. Soares Lavra,⁹ M. D. Sokoloff,⁶⁴ F. J. P. Soler,⁵⁸ A. Solovov,³⁷ I. Solovyev,³⁷ F. L. Souza De Almeida,² B. Souza De Paula,² B. Spaan,¹⁴ E. Spadaro Norella,^{25,p} P. Spradlin,⁵⁸ F. Stagni,⁴⁷ M. Stahl,⁶⁴ S. Stahl,⁴⁷ P. Stefko,⁴⁸ O. Steinkamp,^{49,80} S. Stemmler,¹⁶ O. Stenyakin,⁴³ H. Stevens,¹⁴ S. Stone,⁶⁷ M. E. Stramaglia,⁴⁸ M. Straticiu,³⁶ D. Strelakina,⁸⁰ S. Strovkov,⁸² F. Suljik,⁶² J. Sun,²⁶ L. Sun,⁷² Y. Sun,⁶⁵ P. Svihra,⁶¹ P. N. Swallow,⁵² K. Swientek,³⁴ A. Szabelski,³⁵ T. Szumlak,³⁴ M. Szymanski,⁴⁷ S. Taneja,⁶¹ Z. Tang,³ T. Tekampe,¹⁴ F. Teubert,⁴⁷ E. Thomas,⁴⁷ K. A. Thomson,⁵⁹ M. J. Tilley,⁶⁰ V. Tisserand,⁹ S. T'Jampens,⁸ M. Tobin,⁶ S. Tolc,⁴⁷ L. Tomassetti,^{20,e} D. Torres Machado,¹ D. Y. Tou,¹² M. Traill,⁵⁸ M. T. Tran,⁴⁸ E. Trifonova,⁸⁰ C. Trippl,⁴⁸ A. Tsaregorodtsev,¹⁰ G. Tuci,^{28,t} A. Tully,⁴⁸ N. Tuning,³¹ A. Ukleja,³⁵ D. J. Unverzagt,¹⁶ A. Usachov,³¹ A. Ustyuzhanin,^{41,81} U. Uwer,¹⁶ A. Vagner,⁸² V. Vagnoni,¹⁹ A. Valassi,⁴⁷ G. Valenti,¹⁹ N. Valls Canudas,⁴⁴ M. van Beuzekom,³¹ H. Van Hecke,⁶⁶ E. van Herwijnen,⁸⁰ C. B. Van Hulse,¹⁷ M. van Veghel,⁷⁷ R. Vazquez Gomez,⁴⁵ P. Vazquez Regueiro,⁴⁵ C. Vázquez Sierra,³¹ S. Vecchi,²⁰ J. J. Velthuis,⁵³ M. Veltri,^{21,v} A. Venkateswaran,⁶⁷ M. Veronesi,³¹ M. Vesterinen,⁵⁵ D. Vieira,⁶⁴ M. Vieites Diaz,⁴⁸ H. Viemann,⁷⁵ X. Vilasis-Cardona,⁸³ E. Vilella Figueras,⁵⁹ P. Vincent,¹² G. Vitali,²⁸ A. Vollhardt,⁴⁹ D. Vom Bruch,¹² A. Vorobyev,³⁷ V. Vorobyev,^{42,d} N. Voropaev,³⁷ R. Waldi,⁷⁵ J. Walsh,²⁸ C. Wang,¹⁶ J. Wang,³ J. Wang,⁷² J. Wang,⁴ J. Wang,⁶ M. Wang,³ R. Wang,⁵³ Y. Wang,⁷ Z. Wang,⁴⁹ D. R. Ward,⁵⁴ H. M. Wark,⁵⁹ N. K. Watson,⁵² S. G. Weber,¹² D. Websdale,⁶⁰ C. Weisser,⁶³ B. D. C. Westhenry,⁵³ D. J. White,⁶¹ M. Whitehead,⁵³ D. Wiedner,¹⁴ G. Wilkinson,⁶² M. Wilkinson,⁶⁷ I. Williams,⁵⁴ M. Williams,^{63,68} M. R. J. Williams,⁵⁷ F. F. Wilson,⁵⁶ W. Wislicki,³⁵ M. Witek,³³ L. Witola,¹⁶ G. Wormser,¹¹ S. A. Wotton,⁵⁴ H. Wu,⁶⁷ K. Wyllie,⁴⁷ Z. Xiang,⁵ D. Xiao,⁷ Y. Xie,⁷ H. Xing,⁷¹ A. Xu,⁴ J. Xu,⁵ L. Xu,³ M. Xu,⁷ Q. Xu,⁵ Z. Xu,⁵ Z. Xu,⁴ D. Yang,³ Y. Yang,⁵ Z. Yang,³ Z. Yang,⁶⁵ Y. Yao,⁶⁷ L. E. Yeomans,⁵⁹ H. Yin,⁷ J. Yu,⁷⁰ X. Yuan,⁶⁷ O. Yushchenko,⁴³ K. A. Zarebski,⁵² M. Zavertyaev,^{15,s} M. Zdybal,³³ O. Zenaiev,⁴⁷ M. Zeng,³ D. Zhang,⁷ L. Zhang,³ S. Zhang,⁴ Y. Zhang,⁴⁷ Y. Zhang,⁶² A. Zhelezov,¹⁶ Y. Zheng,⁵ X. Zhou,⁵ Y. Zhou,⁵ X. Zhu,³ V. Zhukov,^{13,39} J. B. Zonneveld,⁵⁷ S. Zucchelli,^{19,b} D. Zuliani,²⁷ and G. Zunica⁶¹

(LHCb Collaboration)

¹Centro Brasileiro de Pesquisas Físicas (CBPF), Rio de Janeiro, Brazil

²Universidade Federal do Rio de Janeiro (UFRJ), Rio de Janeiro, Brazil

³Center for High Energy Physics, Tsinghua University, Beijing, China

⁴School of Physics State Key Laboratory of Nuclear Physics and Technology, Peking University, Beijing, China

⁵University of Chinese Academy of Sciences, Beijing, China

⁶Institute Of High Energy Physics (IHEP), Beijing, China

⁷Institute of Particle Physics, Central China Normal University, Wuhan, Hubei, China

⁸Univ. Grenoble Alpes, Univ. Savoie Mont Blanc, CNRS, IN2P3-LAPP, Annecy, France

- ⁹Université Clermont Auvergne, CNRS/IN2P3, LPC, Clermont-Ferrand, France
- ¹⁰Aix Marseille Univ, CNRS/IN2P3, CPPM, Marseille, France
- ¹¹Jclab, Orsay, France
- ¹²LPNHE, Sorbonne Université, Paris Diderot Sorbonne Paris Cité, CNRS/IN2P3, Paris, France
- ¹³I. Physikalisches Institut, RWTH Aachen University, Aachen, Germany
- ¹⁴Fakultät Physik, Technische Universität Dortmund, Dortmund, Germany
- ¹⁵Max-Planck-Institut für Kernphysik (MPIK), Heidelberg, Germany
- ¹⁶Physikalisches Institut, Ruprecht-Karls-Universität Heidelberg, Heidelberg, Germany
- ¹⁷School of Physics, University College Dublin, Dublin, Ireland
- ¹⁸INFN Sezione di Bari, Bari, Italy
- ¹⁹INFN Sezione di Bologna, Bologna, Italy
- ²⁰INFN Sezione di Ferrara, Ferrara, Italy
- ²¹INFN Sezione di Firenze, Firenze, Italy
- ²²INFN Laboratori Nazionali di Frascati, Frascati, Italy
- ²³INFN Sezione di Genova, Genova, Italy
- ²⁴INFN Sezione di Milano-Bicocca, Milano, Italy
- ²⁵INFN Sezione di Milano, Milano, Italy
- ²⁶INFN Sezione di Cagliari, Monserrato, Italy
- ²⁷Università degli Studi di Padova, Università e INFN, Padova, Padova, Italy
- ²⁸INFN Sezione di Pisa, Pisa, Italy
- ²⁹INFN Sezione di Roma Tor Vergata, Roma, Italy
- ³⁰INFN Sezione di Roma La Sapienza, Roma, Italy
- ³¹Nikhef National Institute for Subatomic Physics, Amsterdam, Netherlands
- ³²Nikhef National Institute for Subatomic Physics and VU University Amsterdam, Amsterdam, Netherlands
- ³³Henryk Niewodniczanski Institute of Nuclear Physics Polish Academy of Sciences, Kraków, Poland
- ³⁴AGH—University of Science and Technology, Faculty of Physics and Applied Computer Science, Kraków, Poland
- ³⁵National Center for Nuclear Research (NCBJ), Warsaw, Poland
- ³⁶Horia Hulubei National Institute of Physics and Nuclear Engineering, Bucharest-Magurele, Romania
- ³⁷Petersburg Nuclear Physics Institute NRC Kurchatov Institute (PNPI NRC KI), Gatchina, Russia
- ³⁸Institute of Theoretical and Experimental Physics NRC Kurchatov Institute (ITEP NRC KI), Moscow, Russia
- ³⁹Institute of Nuclear Physics, Moscow State University (SINP MSU), Moscow, Russia
- ⁴⁰Institute for Nuclear Research of the Russian Academy of Sciences (INR RAS), Moscow, Russia
- ⁴¹Yandex School of Data Analysis, Moscow, Russia
- ⁴²Budker Institute of Nuclear Physics (SB RAS), Novosibirsk, Russia
- ⁴³Institute for High Energy Physics NRC Kurchatov Institute (IHEP NRC KI), Protvino, Russia, Protvino, Russia
- ⁴⁴ICCUB, Universitat de Barcelona, Barcelona, Spain
- ⁴⁵Instituto Galego de Física de Altas Enerxías (IGFAE), Universidade de Santiago de Compostela, Santiago de Compostela, Spain
- ⁴⁶Instituto de Física Corpuscular, Centro Mixto Universidad de Valencia—CSIC, Valencia, Spain
- ⁴⁷European Organization for Nuclear Research (CERN), Geneva, Switzerland
- ⁴⁸Institute of Physics, Ecole Polytechnique Fédérale de Lausanne (EPFL), Lausanne, Switzerland
- ⁴⁹Physik-Institut, Universität Zürich, Zürich, Switzerland
- ⁵⁰NSC Kharkiv Institute of Physics and Technology (NSC KIPT), Kharkiv, Ukraine
- ⁵¹Institute for Nuclear Research of the National Academy of Sciences (KINR), Kyiv, Ukraine
- ⁵²University of Birmingham, Birmingham, United Kingdom
- ⁵³H.H. Wills Physics Laboratory, University of Bristol, Bristol, United Kingdom
- ⁵⁴Cavendish Laboratory, University of Cambridge, Cambridge, United Kingdom
- ⁵⁵Department of Physics, University of Warwick, Coventry, United Kingdom
- ⁵⁶STFC Rutherford Appleton Laboratory, Didcot, United Kingdom
- ⁵⁷School of Physics and Astronomy, University of Edinburgh, Edinburgh, United Kingdom
- ⁵⁸School of Physics and Astronomy, University of Glasgow, Glasgow, United Kingdom
- ⁵⁹Oliver Lodge Laboratory, University of Liverpool, Liverpool, United Kingdom
- ⁶⁰Imperial College London, London, United Kingdom
- ⁶¹Department of Physics and Astronomy, University of Manchester, Manchester, United Kingdom
- ⁶²Department of Physics, University of Oxford, Oxford, United Kingdom
- ⁶³Massachusetts Institute of Technology, Cambridge, Massachusetts, USA
- ⁶⁴University of Cincinnati, Cincinnati, Ohio, USA
- ⁶⁵University of Maryland, College Park, Maryland, USA
- ⁶⁶Los Alamos National Laboratory (LANL), Los Alamos, New Mexico, USA
- ⁶⁷Syracuse University, Syracuse, New York, USA

⁶⁸*School of Physics and Astronomy, Monash University, Melbourne, Australia
(associated with Department of Physics, University of Warwick, Coventry, United Kingdom)*

⁶⁹*Pontifícia Universidade Católica do Rio de Janeiro (PUC-Rio), Rio de Janeiro, Brazil
[associated with Universidade Federal do Rio de Janeiro (UFRJ), Rio de Janeiro, Brazil]*

⁷⁰*Physics and Micro Electronic College, Hunan University, Changsha City, China
(associated with Institute of Particle Physics, Central China Normal University, Wuhan, Hubei, China)*

⁷¹*Guangdong Provincial Key Laboratory of Nuclear Science, Institute of Quantum Matter, South China Normal University, Guangzhou, China (associated with Center for High Energy Physics, Tsinghua University, Beijing, China)*

⁷²*School of Physics and Technology, Wuhan University, Wuhan, China
(associated with Center for High Energy Physics, Tsinghua University, Beijing, China)*

⁷³*Departamento de Física, Universidad Nacional de Colombia, Bogota, Colombia
(associated with LPNHE, Sorbonne Université, Paris Diderot Sorbonne Paris Cité, CNRS/IN2P3, Paris, France)*

⁷⁴*Universität Bonn—Helmholtz-Institut für Strahlen und Kernphysik, Bonn, Germany
(associated with Physikalisches Institut, Ruprecht-Karls-Universität Heidelberg, Heidelberg, Germany)*

⁷⁵*Institut für Physik, Universität Rostock, Rostock, Germany
(associated with Physikalisches Institut, Ruprecht-Karls-Universität Heidelberg, Heidelberg, Germany)*

⁷⁶*INFN Sezione di Perugia, Perugia, Italy (associated with INFN Sezione di Ferrara, Ferrara, Italy)
⁷⁷Van Swinderen Institute, University of Groningen, Groningen, Netherlands*

(associated with Nikhef National Institute for Subatomic Physics, Amsterdam, Netherlands)

⁷⁸*Universiteit Maastricht, Maastricht, Netherlands
(associated with Nikhef National Institute for Subatomic Physics, Amsterdam, Netherlands)*

⁷⁹*National Research Centre Kurchatov Institute, Moscow, Russia [associated with Institute of Theoretical and Experimental Physics NRC Kurchatov Institute (ITEP NRC KI), Moscow, Russia]*

⁸⁰*National University of Science and Technology “MISIS”, Moscow, Russia
[associated with Institute of Theoretical and Experimental Physics NRC Kurchatov Institute (ITEP NRC KI), Moscow, Russia]*

⁸¹*National Research University Higher School of Economics, Moscow, Russia
(associated with Yandex School of Data Analysis, Moscow, Russia)*

⁸²*National Research Tomsk Polytechnic University, Tomsk, Russia [associated with Institute of Theoretical and Experimental Physics NRC Kurchatov Institute (ITEP NRC KI), Moscow, Russia]*

⁸³*DS4DS, La Salle, Universitat Ramon Llull, Barcelona, Spain (associated with ICCUB, Universitat de Barcelona, Barcelona, Spain)
⁸⁴University of Michigan, Ann Arbor, Michigan, USA (associated with Syracuse University, Syracuse, New York, USA)*

[†]daniel.johnson@cern.ch

^aAlso at Università di Genova, Genova, Italy.

^bAlso at Università di Bologna, Bologna, Italy.

^cAlso at Università di Modena e Reggio Emilia, Modena, Italy.

^dAlso at Novosibirsk State University, Novosibirsk, Russia.

^eAlso at Università di Ferrara, Ferrara, Italy.

^fAlso at Università di Milano Bicocca, Milano, Italy.

^gAlso at Università di Bari, Bari, Italy.

^hAlso at Università di Cagliari, Cagliari, Italy.

ⁱAlso at Laboratoire Leprince-Ringuet, Palaiseau, France.

^jAlso at Università di Roma Tor Vergata, Roma, Italy.

^kAlso at Universidade Federal do Triângulo Mineiro (UFMT), Uberaba-MG, Brazil.

^lAlso at AGH—University of Science and Technology, Faculty of Computer Science, Electronics and Telecommunications, Kraków, Poland.

^mAlso at Università di Siena, Siena, Italy.

ⁿAlso at Università di Padova, Padova, Italy.

^oAlso at Scuola Normale Superiore, Pisa, Italy.

^pAlso at Università degli Studi di Milano, Milano, Italy.

^qAlso at MSU—Iligan Institute of Technology (MSU-IIT), Iligan, Philippines.

^rAlso at Università di Firenze, Firenze, Italy.

^sAlso at P.N. Lebedev Physical Institute, Russian Academy of Science (LPI RAS), Moscow, Russia.

^tAlso at Università di Pisa, Pisa, Italy.

^uAlso at Università della Basilicata, Potenza, Italy.

^vAlso at Università di Urbino, Urbino, Italy.